Electronic Supplementary Material (ESI) for Physical Chemistry Chemical Physics

Supporting Online Materials: Nature of proton transport in a water-filled carbon nanotube and in liquid water

Ji Chen,[†] Xin-Zheng Li,[*,‡,¶] Qianfan Zhang,[‡] Angelos Michaelides,[¶] and Enge Wang[*,†]

ICQM and School of Physics, Peking University, Beijing 100871, P. R. China, School of Physics, Peking University, Beijing 100871, P. R. China, and Thomas Young Centre, London Centre for Nanotechnology and Department of Chemistry, University College London, London WC1E 6BT, U.K.

E-mail: xzli@pku.edu.cn; egwang@pku.edu.cn

Outline

In the main manuscript, we have shown that the key difference between proton transport (PT) in bulk liquid water and in a water-filled carbon nanotube is in the solvent reorganization and that the excess proton is best described as a fluxional defect in both systems. In this supporting online material, we discuss the validity of the simulations from which these conclusions were drawn. The accuracy of the electronic structures we have chosen for the molecular dynamics (MD) and path-integral molecular dynamics (PIMD) simulations is analyzed in S.I. In S.II, we check the

[*]To whom correspondence should be addressed
[†]Peking University, address 1
[‡]Peking University, address 2
[¶]University College London

convergence of the MD and PIMD simulations and compare their auto-correlation functions with those reported in an earlier study.[1] The "limiting" forms of the excess proton's hydration state associated with the evolution of $|\delta_2| - |\delta_1|$ (Figure 4 of the main manuscript) are analyzed in S.III. Compared with the fluxional defect mechanism, PT in bulk liquid water is also often described in terms of spatial pair dancing in many theoretical simulations.[2,3] In S.IV, we discuss the validity of this spacial pair dancing mechanism in our *ab initio* MD simulation of the bulk liquid water and how the quantum nuclear motion impacts on it.

S.I Accuracy of the electronic structures

The main procedure we adopted to check the quality of the PBE-based MD simulations was to randomly select ten snapshots from the MD simulation and then to compare the relative total energies of these snapshots through single point total energy calculations with various settings. Specifically, we show results with different plane-wave energy cut-offs in Figure S1 (a) and with various *k*-meshes in Figure S1 (b). Any potential role of van der Waals forces in this system was examined in a similar manner using the newly proposed optB88-vdW functional[4,5] within the vdW-DF scheme[6,7] (Figure S1 (c)). As can be seen from Figure 1 the relative energies of the ten snapshots span about a range of 2 eV, with snapshot 1 set to zero and the other snapshots aligned in order of ascending total energy. It can be seen that the relative energies of the various snapshots is very well preserved no matter what settings are used. Indeed, compared with the total energy differences between the snapshots which are on the eV scale, the energy differences between results obtained from the settings we have chosen in the MD simulations and the more accurate ones (higher energy cut-off, denser *k*-mesh) as well as the vdW-DF calculations are only a few meV.

Besides van der Waals interactions, another possible source of error related to the use of PBE in the simulations reported is the so-called self-interaction error, which could lead to the PBE proton transfer barrier being underestimated. This can be examined by comparing the relative total

energies obtained with PBE and those obtained using more expensive hybrid exchange-correlation functionals that contain a fraction of Hartree-Fock exact exchange.[8–16] Here we have done this by comparing the relative energies of the same ten snapshots extracted from the PBE-based MD simulation through single point calculations with PBE, PBE0 and HSE. The results of this analysis are also shown in Figure S1 (c)). Again we see that the relative energies of the various states obtained from PBE are well-preserved, and the differences in total energies between the various snapshots obtained from PBE and PBE0 are always within 10% of each other. Considering the fact that such a comparison contains noise unrelated to PT, we have performed a further analysis focusing on the transfer of one proton along a HB. One snapshot from the simulation where the excess proton clearly belongs to one oxygen is chosen first (labeled as snapshot1 in Figure S2 (a)). Then, we move the excess proton along its HB toward the corresponding HB acceptor until it arrives at its symmetric site (labeled as snapshot2 in Figure S2 (b)). The corresponding OH bond length is taken as the x coordinate. We plot the change of the whole system's total energy as a function of R_{OH} and compare the results obtained from the PBE, vdW-DF (optB88-vdW), HSE, and PBE0 calculations. Since other atoms don't relax upon moving the excess proton, the system's total energy increases with R_{OH}. The differences between PBE and vdW-DF are smaller than 5 meV. The differences between HSE and PBE0 are also within 1 meV. The differences between PBE and hybrid PBE0 (HSE) results are smaller than 20 meV. This is within 10% of the energy window explored, comparable to the thermal fluctuation at room temperature, and smaller than the corresponding zero-point energy along such intermediate strength HB. Therefore, we believe the electronic structures we have used in our simulations accurately reproduce the actual Born-Oppenheimer potential energy surface, which ensures that the nuclei move in the proper manner.

S.II MD and PIMD calculations

One conclusion we have drawn in the main manuscript for the 1D PT is that the most active proton along the shortest hydrogen bond feels no barrier upon including the quantum nuclear effects. In

PIMD simulations, the results must be converged with respect to the number of replicas (beads). Here we report results of such a test by comparing the free-energy profiles for the most active proton calculated from the MD simulation and the PIMD simulations using different number of beads (Figure S3). It is clear that the conclusion we have drawn in the main manuscript is robust to the number of beads we have chosen in the PIMD simulations. Using classical nuclei, the most active proton feels a barrier of $\sim$2 meV, in good agreement with what has been reported in an earlier study.[17] This barrier is washed out upon including the quantum nuclear effects.

To check the dependence of the results on the length of the water chain, we performed another MD simulation for a large system using a 19.7Å long carbon nanotube which contains 8 water molecules plus one excess proton. Figure S4 shows the evolution of $|\delta_2| - |\delta_1|$ in this simulation compared with that using 6 water molecules. Similar behavior is observed in both simulations, *i.e.* the hydration state of the excess proton interconverts quickly between idealized models, leaving both of them exist only in the limiting sense. Therefore, the picture presented in the main manuscript is insensitive to the length of the CNT and the water chain used in the simulation. Besides this, one may also wonder the radius dependence of the picture presented. As our main finding is that the 1D PT benefits from a favorable pre-alignment of water molecules, as long as the confinement is strong enough to ensure this 1D constraint, this main finding should be unchanged.

In an earlier study,[1] the auto-correlation function for the position of the excess proton ($C(t)$) was reported for an *ab initio* MD simulation of one excess proton along a 1D water chain in a carbon nanotube. We have calculated the same quantity for all the simulations we have reported. The results are shown in Figure S5. The curve corresponding to the MD simulations of the same system nicely reproduces the one reported in the earlier study.[1] After 2.5 ps, $C(t)$ decrease to a value below 0.4, which also guarantees the sampling efficiency of the simulations.

S.III Limiting form of the excess proton's hydration state

In the main manuscript, we have assigned the excess proton's hydration state with small $|\delta_2| - |\delta_1|$ to $H_7O_3^+$ complex and that with large $|\delta_2| - |\delta_1|$ to Zundel. To analyze the "limiting" form of it associated with the evolution of $|\delta_2| - |\delta_1|$ from a rigorous perspective, we take a procedure similar to two earlier studies[18,19] and choose two windows for $|\delta_2| - |\delta_1|$. The small $|\delta_2| - |\delta_1|$ window uses the spatial configuration of the system visited with this value smaller than 0.2 Å. The large $|\delta_2| - |\delta_1|$ window uses those when it is larger than 0.3 Å. Using these structures, we have plotted the radial distribution functions (RDFs) of R_{OH} from the pivot oxygen O^p. We take out contributions from the non-hydrogen-bonded proton to get rid of its noise. The results are shown in Figure S6. The RDF with small $|\delta_2| - |\delta_1|$ shows a single peak at $\sim$1.1 Å, corresponding to a complex with $H_7O_3^+$-like structure. The RDF with large $|\delta_2| - |\delta_1|$ shows two peaks. The one at short OH comes from the neighboring HB of the Zundel complex where the HB is weak and the position of the peak corresponds to a covalent bond (inset of Figure 4 (a) in the main manuscript). The one at longer OH comes from the Zundel complex itself where the proton is equally shared by the two oxygen atoms. The coordination numbers, meanwhile, show a similar trend. In the Zundel complexes, the hydrogen atom lying on the neighboring HB of $H_5O_2^+$ contributes to a fast increase to 1 at short R_{OH}. The further increase of this number to 2, on the other hand, happens much later due to the fact that the proton in the Zundel complex is equally shared with relatively large R_{OH} at 1.2 Å. This behavior, however, is absent for the coordinate number with small $|\delta_2| - |\delta_1|$. Therefore, it is clear that the configurations with large $|\delta_2| - |\delta_1|$ shown in Figure 4 (a) of the main manuscript correspond to Zundel-like structures and those with small $|\delta_2| - |\delta_1|$ correspond to $H_7O_3^+$-like ones. Although PIMD provides rigorous only statistical information, the often appeared situation when $H_7O_3^+$ and Zundel-like complexes interconvert between one another still indicates that it is inappropriate to describe the system as comprised mainly of one dominant idealized structure or another. Rather, the fluxional defect picture for the hydration state of an excess proton in bulk liquid water[18] should be extended to this nanoconfined system.

S.IV Spatial pair dancing

In above, we have demonstrated that PT in both bulk liquid water and 1D water chain should be best described in terms of a fluxional defect, which is consistent with an earlier *ab initio* PIMD simulation of PT in bulk liquid water.[18] In contrast to this, many theoretical simulations have also shown that a spatial pair dancing mechanism is more appropriate to describe this PT process in bulk liquid water.[2,3] To shed light on this discrepancy, we follow the same procedure as that has been used in those simulations favouring special pair dancing and label the oxygen which owns three proton as O_0 and the oxygen which shares the most active proton with it as O_{1x}. Then, we plot the evolution for the identity of these two oxygen atoms during a certain period of the simulation time in Figure S7. The panels a) and c) describe results from the *ab initio* MD simulation with classical nuclei and the panels d) and f) describe results from the *ab initio* PIMD simulation where the quantum nuclear motion has been taken care of. In addition to these, the evolution of δ, which is the difference between the two OH bond lengths to which a certain proton is subjected to for the most active proton from these two sets of simulations, is also plotted in panels b) and e). When the excess proton is hydrated as Zundel, this δ is small. When it is hydrated as Eigen, this δ is large. We first look as the upper three panels. When O_0 stays stably on one oxygen atom during the period of ps, O_{1x} switches identity and δ is relatively large. The hydration state of the excess proton is Eigen and the excess proton dances between the neighboring HBs. This is in agreement with the special dancing mechanism. However, upon including the quantum nuclear effects, O_0 dances quickly between different atoms and the fluxional defect picture clearly becomes more appropriate.

The above analysis indicates that the treatment of the quantum nuclear motion can be a possible source for the discrepancy between our picture and that of the special pair dancing. But we acknowledge that this can't be all. The impact of quantum nuclear effects sensitively depends on the shape of the Born-Oppenheimer potential energy surface upon which the quantum nuclear effects are evaluated.[20] One needs to acknowledge that most simulations favouring the special pair dancing picture are based on the Multi-State Emperical Valence Bond (MS-EVB) method, which

provides different Born-Oppenheimer Potential Energy Surface for the propogation of the nuclei from the *ab initio* method used here. This issue obviously needs a systematic study in the future, which is beyond the scope of our current study.

References

(1) Dellago, C.; Naor, M. M.; Hummer, G. *Phys. Rev. Lett.* **2003**, *90*, 4.

(2) Markovitch, O.; Chen, H. N.; Izvekov, S.; Paesani, F.; Voth, G. A.; Agmon, N. *J. Phys. Chem. B* **2008**, *112*, 9456–9466.

(3) Xu, J. Q.; Zhang, Y.; Voth, G. A. *J. Phys. Chem. Lett.* **2011**, *2*, 81–86.

(4) Klimeš, J.; Bowler, D. R.; Michaelides, A. *J. Phys.: Condens. Matter* **2010**, *22*, 022201.

(5) Klimeš, J.; Bowler, D. R.; Michaelides, A. *Phys. Rev. B* **2011**, *83*, 195131.

(6) Dion, M.; Rydberg, H.; Schroder, E.; Langreth, D. C.; Lundqvist, B. I. *Phys. Rev. Lett.* **2004**, *92*, 246401.

(7) Langreth, D. C.; Dion, M.; Rydberg, H.; Schroder, E.; Hyldgaard, P.; Lundqvist, B. I. *Int. J. Quant. Chem.* **2005**, *101*, 599.

(8) Heyd, J.; Scuseria, G. E.; Ernzerhof, M. *J. Chem. Phys.* **2003**, *118*, 8207.

(9) Adamo, V.; Barone, V. *J. Chem. Phys.* **1999**, *110*, 6158.

(10) Zhao, Y.; Lynch, B. J.; Truhlar, D. G. *J. Phys. Chem. A* **2004**, *108*, 2715.

(11) Baker, J.; Andzelm, J.; Muir, M.; Taylor, P. R. *Chem. Phys. Lett.* **1995**, *237*, 53.

(12) Barone, V.; Orlandini, L.; Adamo, C. *Chem. Phys. Lett.* **1994**, *231*, 295.

(13) Barone, V.; Adamo, C.; Mele, F. *Chem. Phys. Lett.* **1996**, *249*, 290.

(14) Barone, V.; Adamo, C. *Int. J. Quantum Chem.* **1997**, *61*, 443.

(15) VandeVondele, J.; Sprik, M. *Phys. Chem. Chem. Phys.* **2005**, *7*, 1363.

(16) Zhang, Q. F.; Wahnström, G.; E., B. M.; Gao, S. W.; Wang, E. G. *Phys. Rev. Lett.* **2008**, *101*, 215902.

(17) Cao, Z.; Peng, Y. X.; Yan, T. Y.; Li, S.; Li, A. L.; Voth, G. A. *J. Am. Chem. Soc.* **2010**, *132*, 11395–11397.

(18) Marx, D.; Tuckerman, M. E.; Hutter, J.; Parrinello, M. *Nature* **1999**, *397*, 601–604.

(19) Tuckerman, M. E.; Marx, D.; Parrinello, M. *Nature* **2002**, *417*, 925–929.

(20) Li, X. Z.; Walker, B.; Michaelides, A. *Proc. Natl. Acad. Sci. USA* **2011**, *108*, 6369.

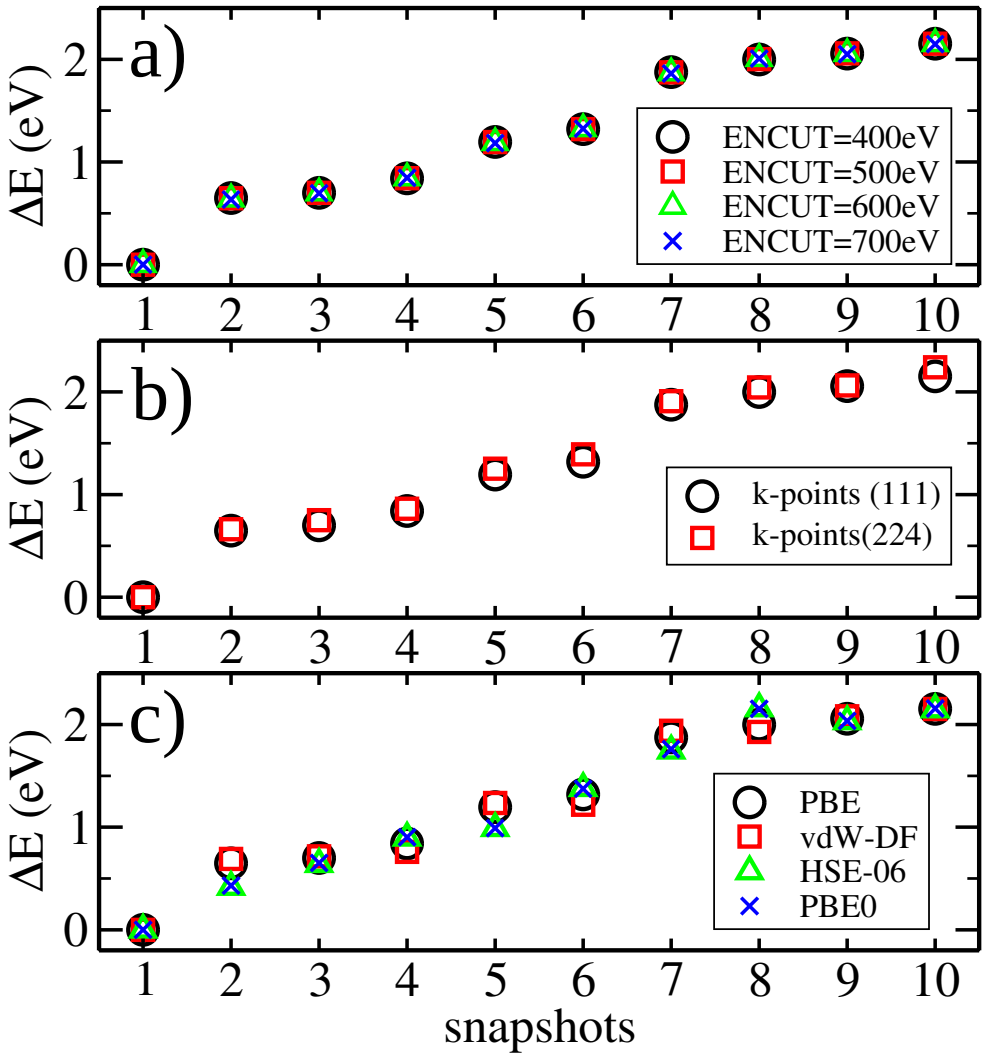

Figure S1: Relative total energy of ten randomly selected snapshots from the PBE-based MD simulation of a water-filled carbon nanotube. The lowest energy snapshots (snapshot 1) is set to zero. In panel (a) we show the sensitivity of the results to different plane-wave energy cut-off (400 eV, black circle; 500 eV, red square; 600 eV, green triangle; 700 eV, blue cross). In panel (b) we show the sensitivity of the results to different *k*-meshes (Γ-point only in black square and the (224) mesh in red circle). In panel (c) we compare results obtained using different exchange-correlation functionals.

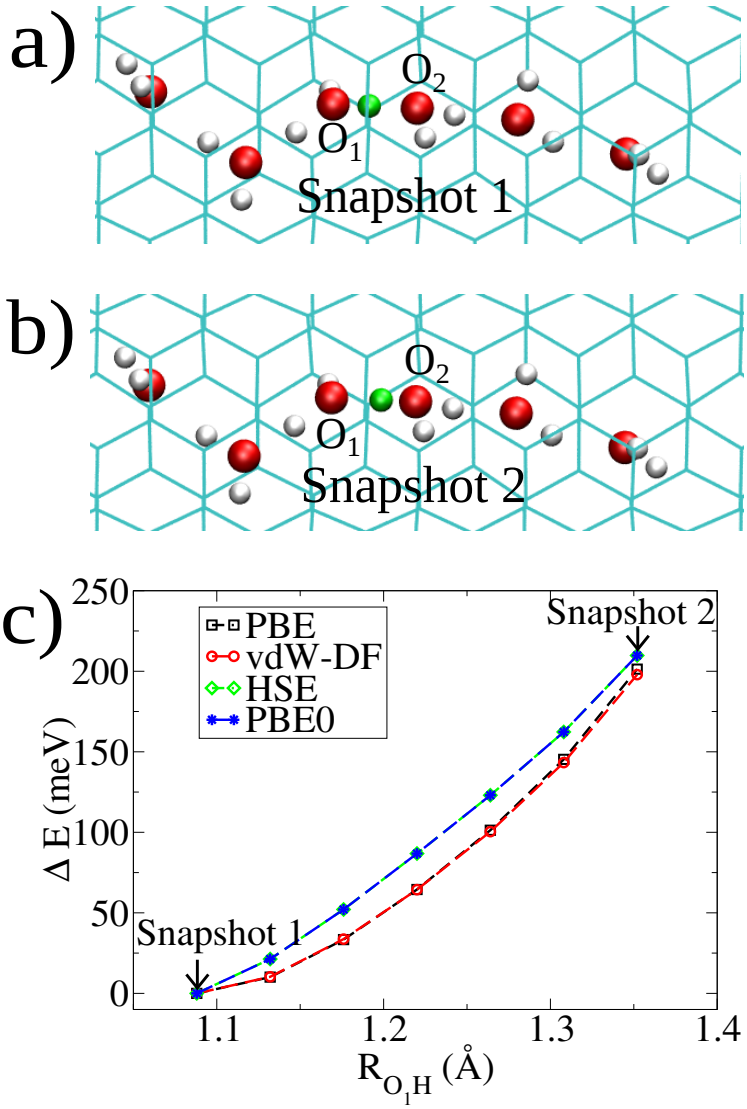

Figure S2: Total energy profile for PT along a HB within a water-filled carbon nanotube. Panel a) shows a snapshot of the system when the excess proton (in green) clearly belongs to O_1. Then, we move it along the HB toward O_2 until it arrives at its symmetric site (b, other atoms unmoved). Panel c) shows the change of the system's total energy as a function of R_{O_1H} for several different exchange-correlation functionals.

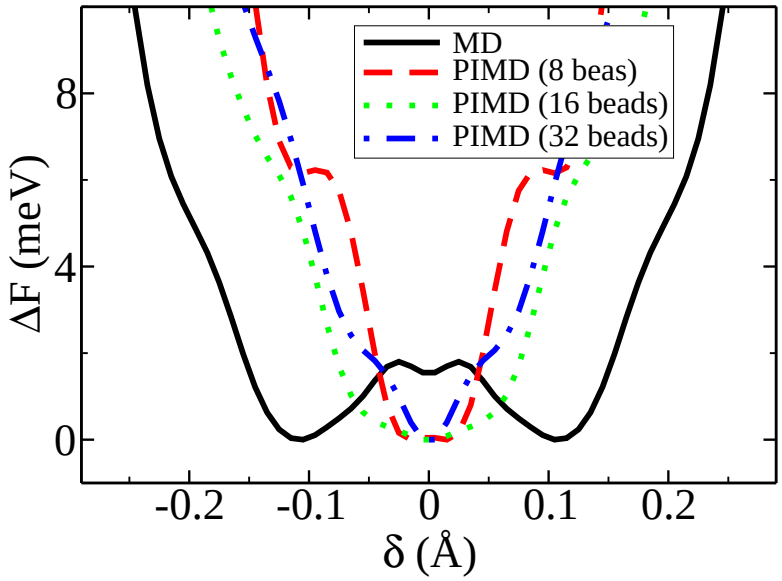

Figure S3: Free-energy profile calculated from $\Delta F(\delta) = -k_{\mathrm{B}} T ln(P[\delta])$ in different simulations (MD, black solid line; 8 beads PIMD, red dashed line; 16 beads PIMD, green dotted line; 32 beads PIMD, blue dotted dashed line). P is the probability as a function of δ on the most active HB.

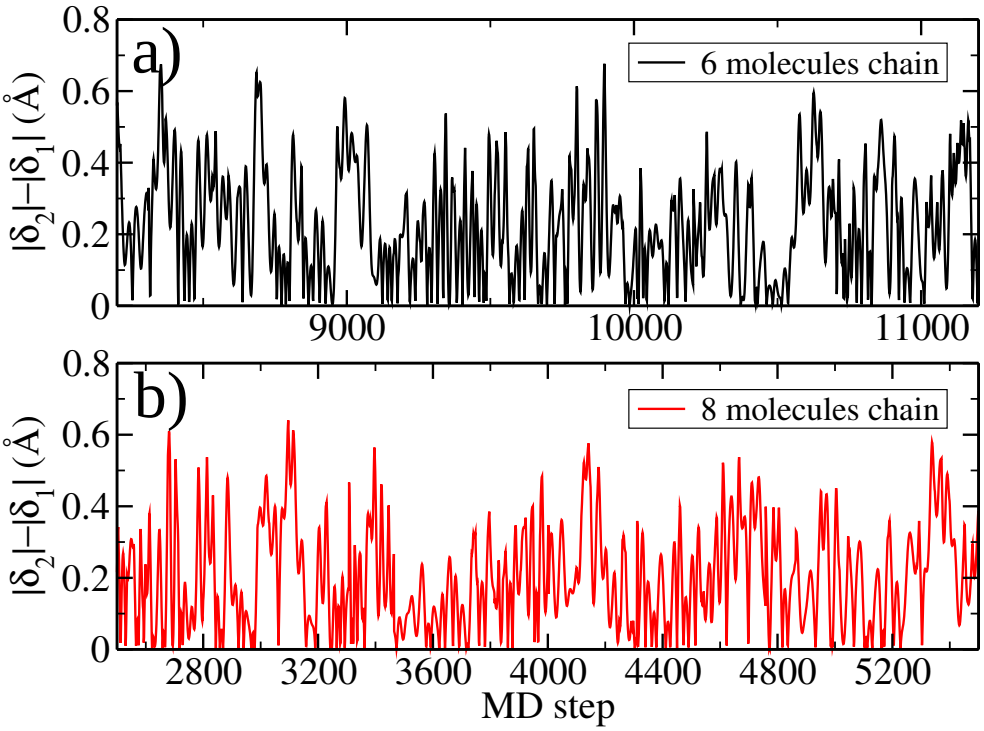

Figure S4: Evolution of $|\delta_2| - |\delta_1|$ in the MD simulation using a water chain containing 6 water molecules (panel a) and 8 water molecules (panel b). Configurations when $|\delta_2| - |\delta_1|$ is large and small quickly interconvert between each other. Leaving idealized hydration states of the excess proton with "limiting" value of this quantity exist only in the limiting sense.

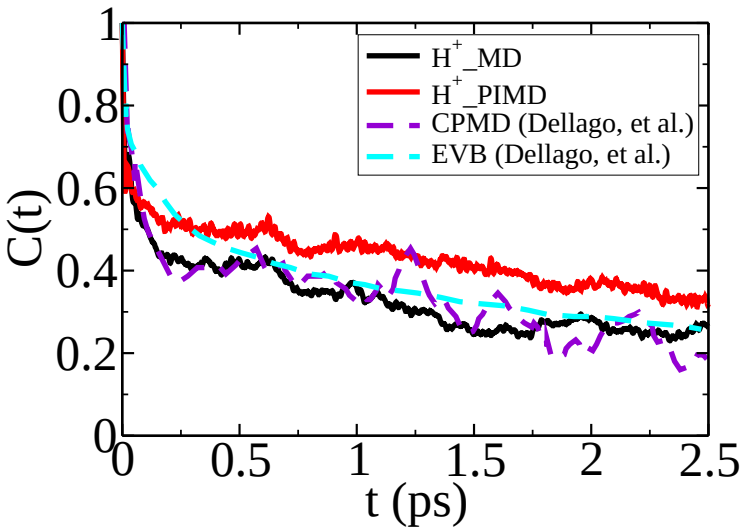

Figure S5: Time auto-correlation function *C*(t) obtained MD and PIMD simulations. black solid line, MD simulation for an excess proton; red solid line, PIMD simulation for an excess proton; violet dashed line, CPMD result extracted from an earlier study;[1] cyan dashed line, empirical valence bond (EVB) result extracted from that study.[1]

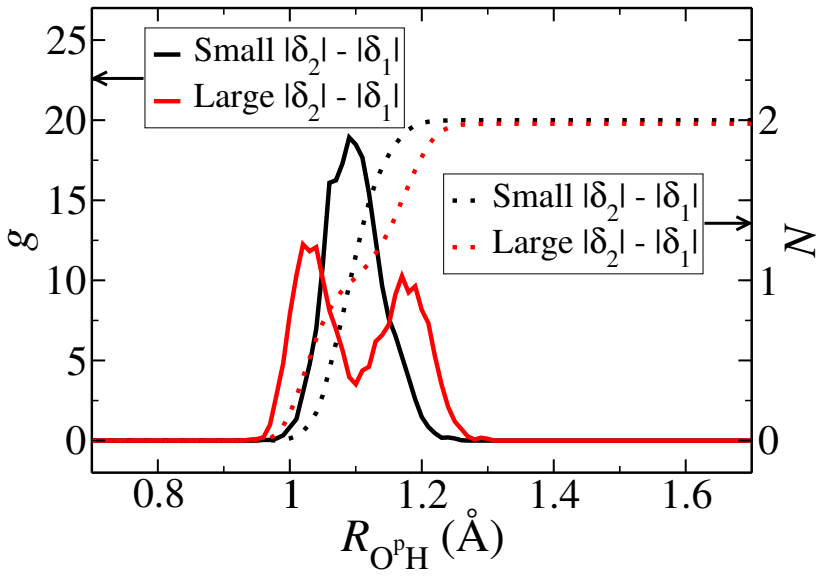

Figure S6: Radial distribution functions g (solid lines, scale on left) from and coordination numbers N (dotted lines, scale on right, number of neighboring H atoms) of the pivot oxygen O^p as functions of R_{O^pH}. Contributions from the non-hydrogen-bonded proton were taken out to get rid of its noise. Lines in red use spatial configurations with $|\delta_2| - |\delta_1| > 0.3$Å. Lines in black use spatial configurations with $|\delta_2| - |\delta_1| < 0.2$Å.

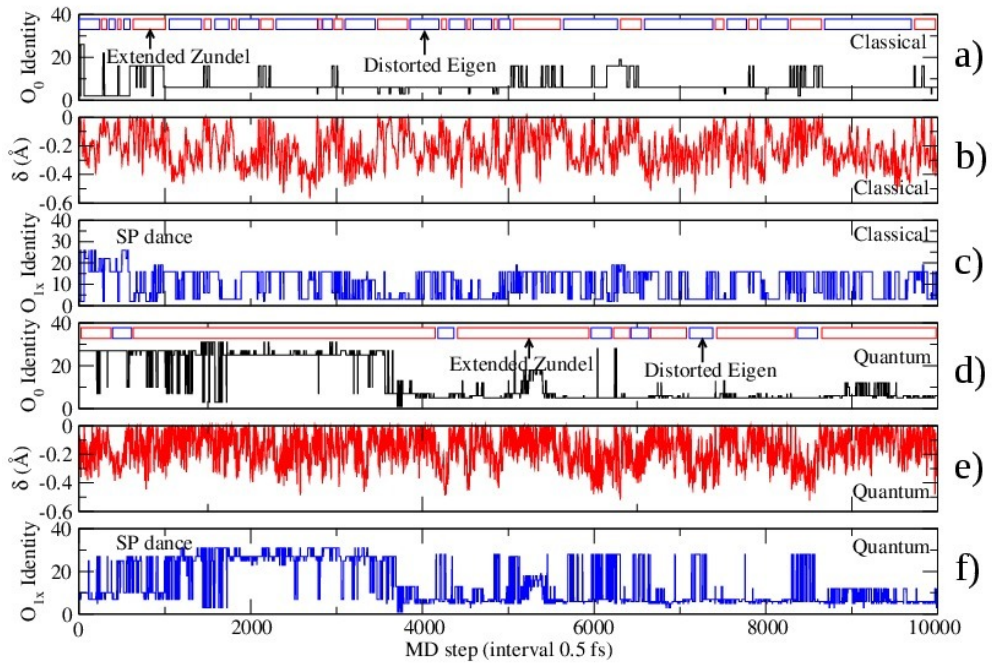

Figure S7: O_0 is the oxygen atom which owns three hydrogen during each simulation step of bulk liquid water. O_{1x} is the oxygen which shares the most active proton with it. δ is the difference between the two OH bond lengths on the most active HB. Panels a) and d) describe the evolution of O_0's identity in the *ab initio* MD and PIMD simulations respectively. Panels b) and e) describe the evolution of δ in the *ab initio* MD and PIMD simulations respectively. And panels c) and f) describe the evolution of O_{1x}'s identity in the *ab initio* MD and PIMD simulations respectively. The special dancing picture is clear in the MD simulation, but significantly weakened in the PIMD simulation.